Heliyon 8 (2022) e10513

Contents lists available at ScienceDirect

Heliyon

journal homepage: www.cell.com/heliyon

Research article

Distinct cell proliferation patterns underlying the development of defensive crests in *Daphnia longicephala*

Annette Graeve [a], Joshua Huster [a], Deria Görl [a], Ioanna Ioannidou [a], Rocio Gómez [b], Linda C. Weiss [a,*]

[a] Department of Animal Ecology, Evolution and Biodiversity, Ruhr-University Bochum, Bochum, Germany
[b] Cell Biology Unit, Department of Biology, Universidad Autónoma de Madrid, Madrid, Spain

ARTICLE INFO

Keywords:
Daphnia
Predation
Inducible defense
Phenotypic plasticity
DNA replication
Cell cycle
Proliferation

ABSTRACT

The freshwater crustacean *Daphnia* is well known for its expression of morphological defenses in the presence of predators. Research into this phenomenon has mostly centered on the ecology and evolution of *Daphnia* defenses; information is limited on the cellular mechanisms that underlie site-specific tissue growth. We aimed to determine these cellular mechanisms, specifically those associated with the development of defensive crests in *D. longicephala*. With the help of a cell-proliferation assay we monitored changes in the epidermal tissue of naïve and predator-exposed *D. longicephala*. Based on our results, we propose that cell division is delayed in favor of cell growth, which results in crest formation. Further, we identify specific regions of proliferative activity in a time-dependent manner. Defense development starts in the ventral region, before extending in the cranial and then dorsal directions. We demonstrate that these cellular changes begin as early as 2 h after predator exposure. Our results provide new insights into the cellular processes underlying morphological defense expression in *Daphnia*.

1. Introduction

Predation is a major selective agent; some prey species have evolved the ability to defend from predators through the expression of inducible defenses. Such defenses can manifest morphologically (Grant and Bayly, 1981; Krueger and Dodson, 1981; Tollrian, 1990), life-history shifts (Macháček, 1991; Stibor and Luning, 1994) or behaviorally (Dodson et al., 1997). Freshwater crustaceans of the genus *Daphnia* are well known for their ability to develop a variety of adaptive morphological defenses, with some forms appearing in the head region (Tollrian and Harvell, 1999). Examples include helmets in *D. cucullata* (Tollrian, 1990), head spines in *D. lumholtzi* (Tollrian and Dodson, 1999), neckteeth in *D. pulex* (Krueger and Dodson, 1981; Tollrian, 1993) and crests in *D. longicephala* (Barry, 2000; Grant and Bayly, 1981; Weiss et al., 2015b). Each of these differs in size and shape, reflecting the differing predation threats that *Daphnia* species experience. The pointed spines expressed in the anterior head region of *D. lumholtzi* can extend several hundred micrometers (Graeve et al., 2021b), while *D. pulex* neckteeth are relatively small and limited to the neck region (Krueger and Dodson, 1981). Crests in *D. longicephala* can reach a significant size and cover the whole head area from ventrally, starting with an elongation of the rostrum, to dorsally, where the crest extends to form a disc-like head shape (Horstmann et al., 2018). Defended *D. longicephala* are less likely to be consumed by their natural Notonectidae predators (Barry and Bayly, 1985; O'Brien and Vinyard, 1978). Although the ecology and evolution of these morphological defenses in *Daphnia* have been intensely studied (Jeschke et al., 2008; Weiss and Tollrian, 2018), there is only limited information on the cellular mechanisms underlying their expression. Defense development is triggered upon the perception via the antennules of predator-specific chemical cues, known as kairomones (Weiss et al., 2015b). Kairomone perception then activates a signaling cascade involving cholinergic, dopaminergic, glutamatergic and GABAergic agents (Miyakawa et al., 2010, 2015; Oda et al., 2011; Weiss et al., 2012a, 2015a). Neuronal rewiring and structural plasticity in the central neuropils precede measurable defense expression (Graeve et al., 2021a). However, the cellular changes that lead to the extensive tissue growth required to form morphological defenses are still elusive. In general, tissues are formed of specialized cells that perform one or more functions (Baker et al., 1976). To develop morphological defenses, tissues like the epidermis have to change their appearance, e.g. through growth. Tissue growth is based on cell proliferation, which comprises cell division and cell growth (Hietakangas and Cohen, 2009; Thompson, 2010). Cells

* Corresponding author.
E-mail address: linda.weiss@rub.de (L.C. Weiss).

https://doi.org/10.1016/j.heliyon.2022.e10513
Received 27 January 2022; Received in revised form 2 May 2022; Accepted 26 August 2022

progress from the G1 phase (the growth phase), to the S phase (DNA synthesis phase), the G2 phase (further growth and preparation for mitosis) and the M phase (mitosis, in which the mother cell divides into two daughter cells) (Matthews et al., 2022). Cell division alone increases cell numbers but not necessarily tissue volume. This is because the daughter cells will each be only half the size of the mother cell (Hietakangas and Cohen, 2009; Zhang et al., 2000). Therefore, cells increase in volume mostly during the G1 phase before division (Hartwell and Weinert, 1989).

In this study, we aimed to elucidate the cellular mechanisms within the epidermis that underlie crest expression in *D. longicephala*. We hypothesized that cell proliferation is critical for the development of defensive morphological features. Our main objective was to determine cell proliferation patterns in the cephalic integument of *Daphnia* that changes shape and develops a crest-like structure in response to *Notonecta* chemical cues (M. J. Barry, 2000; Weiss et al., 2015b). The integument itself consists of different cuticle layers that are secreted by the underlying epidermal cells and interconnected by the extracellular matrix (Kruppert et al., 2017; Stevenson, 1985).

We examined premitotic (S-phase), mitotic (M-phase) and postmitotic (G1-phase) phases using a cell-proliferation assay among predator-exposed and naïve *D. longicephala* at different points in time during a 72-hour period (a period in which defensive strategies are expressed). Furthermore, we investigated changes in cell density within the crest by conducting cell counts in three areas of the epidermal head tissue. This allowed us to determine the epidermal proliferation patterns in naïve and predator-exposed *D. longicephala* that underlie crest expression.

2. Results

We analyzed cell proliferation patterns underlying *Notonecta*-induced crest development in *D. longicephala*, by monitoring DNA replication (via 5-ethynyl-2′-deoxyuridine [EdU] labelling) and cell counts in selected head regions.

2.1. Morphological defense expression

Twenty-four hours after predator exposure, morphological defenses were not significantly expressed: crest height ($t = -1.51$; $df = 63.737$, $P = 0.25$) and width ($t = -0.297$; $df = 65.389$, $P = 0.77$) were not significantly different between the predator-exposed and naïve groups. However, defense expression was significantly different at 48 h (crest height: $t = -2.29$; $df = 107.67$, $P = 0.024$; crest width: $t = -2.328$; $df = 107.29$, $P = 0.022$) and 72 h (crest height: $t = -2.5$; $df = 54.69$, $P = 0.014$; crest width: $t = -2.187$; $df = 59.99$, $P = 0.03$) after predator exposure (Figure 1).

2.2. EdU incorporation pattern

We analyzed EdU incorporation patterns in the whole head tissue over time. We observed a distinct chronological pattern in which EdU-labeled cells were found in the head tissue in naïve and predator-exposed *D. longicephala*. EdU-labeled cells were absent from organisms in both treatments at the beginning of the experiment (0 h). After 2 h, EdU-labeled cells were only found in the tip of the rostrum (Figure 2A–C) in naïve *D. longicephala*. At 24 h in naïve *D. longicephala*, the number of EdU-labeled cells increased, and were also detected cranially and dorsally, this was not observed as strongly in predator-exposed animals (Figure 2G–L). At 72 h, we observed a similar distribution of EdU-labeled cells in naïve and predator-exposed *D. longicephala*. In both treatments at 72 h, the staining pattern in the cranial and dorsal tissue differed from the pattern in the rostrum. Whereas EdU-labeled cells were evenly distributed in the rostral area, they were mainly observed on the distal rim of the cranial and dorsal areas (Figure 2M–R).

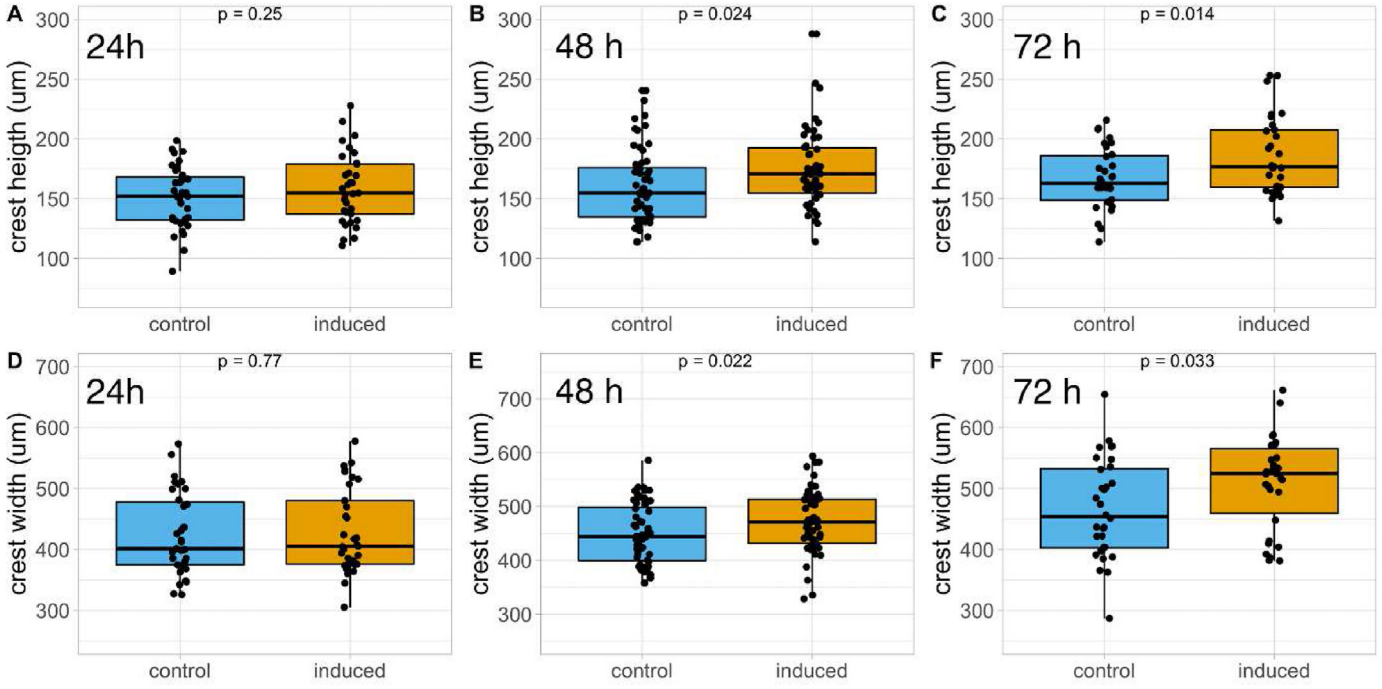

Figure 1. *Notonecta*-induced morphological defense expression over time. A: 24 h after predator exposure, crest height was not significantly increased compared with naïve *D. longicephala*. B, C: Crest height was significantly increased 48 h (B) and 72 h (C) following predator exposure. D: 24 h after predator exposure, crest width was not significantly increased compared with naïve *D. longicephala*. E, F: Crest width was significantly increased at 48 h (E) and 72 h (F) after predator exposure. Boxplots show median (middle line) and 25th to 75th percentiles (box); whiskers show the highest and lowest values within 1.5× the interquartile range (1.5× below the 25th percentile and 1.5× above the 75th percentile). Dots display raw data. *P*-values of t-test statistics are displayed.

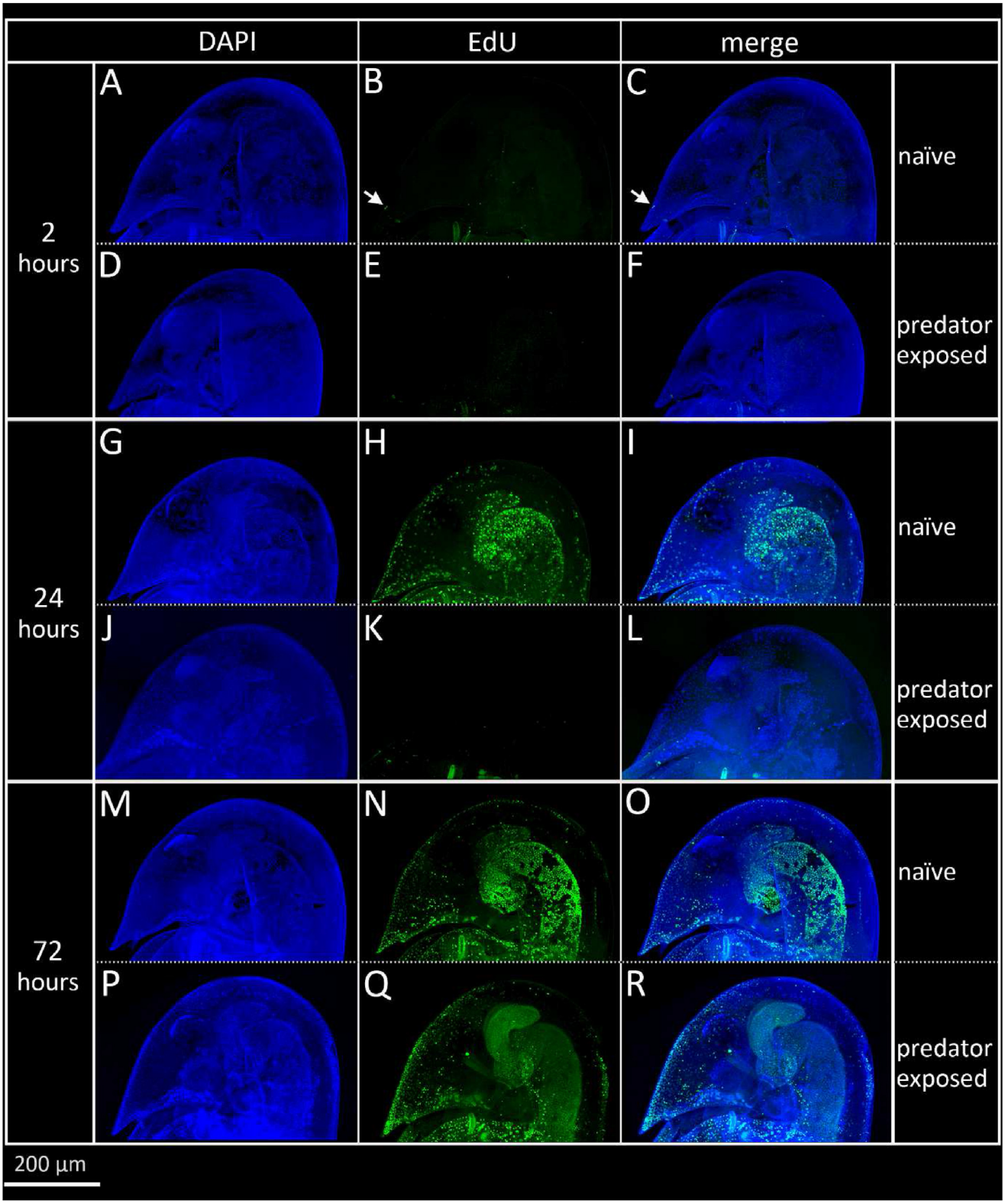

Figure 2. Examples of nuclear staining patterns of DAPI and EdU in predator-exposed and naïve *D. longicephala* after 2 h, 24 h and 72 h. The left column shows DAPI, the middle column shows EdU fluorescence and the right column shows the two channels combined. A–C: Naïve *D. longicephala* after 2 h. Two EdU-labeled nuclei can be seen in the rostrum (white arrow). D–F: *D. longicephala* after 2 h predator exposure. No EdU-labeled nuclei are observable. G–I: Naïve *D. longicephala* after 24 h. EdU-labeled nuclei are found throughout the head tissue, with the strongest mitotic activity in the rostrum (H). J–L: *D. longicephala* after 24 h predator exposure, few EdU-labeled cells are observable. M–O: Naïve *D. longicephala* after 72 h predator exposure. EdU-labeled nuclei are observable throughout the head tissue, with the strongest mitotic activity in the rostrum (N). P–R: *D. longicephala* after 72 h predator exposure. EdU-labeled nuclei are observable throughout the head tissue, with the strongest mitotic activity in the rostrum (Q).

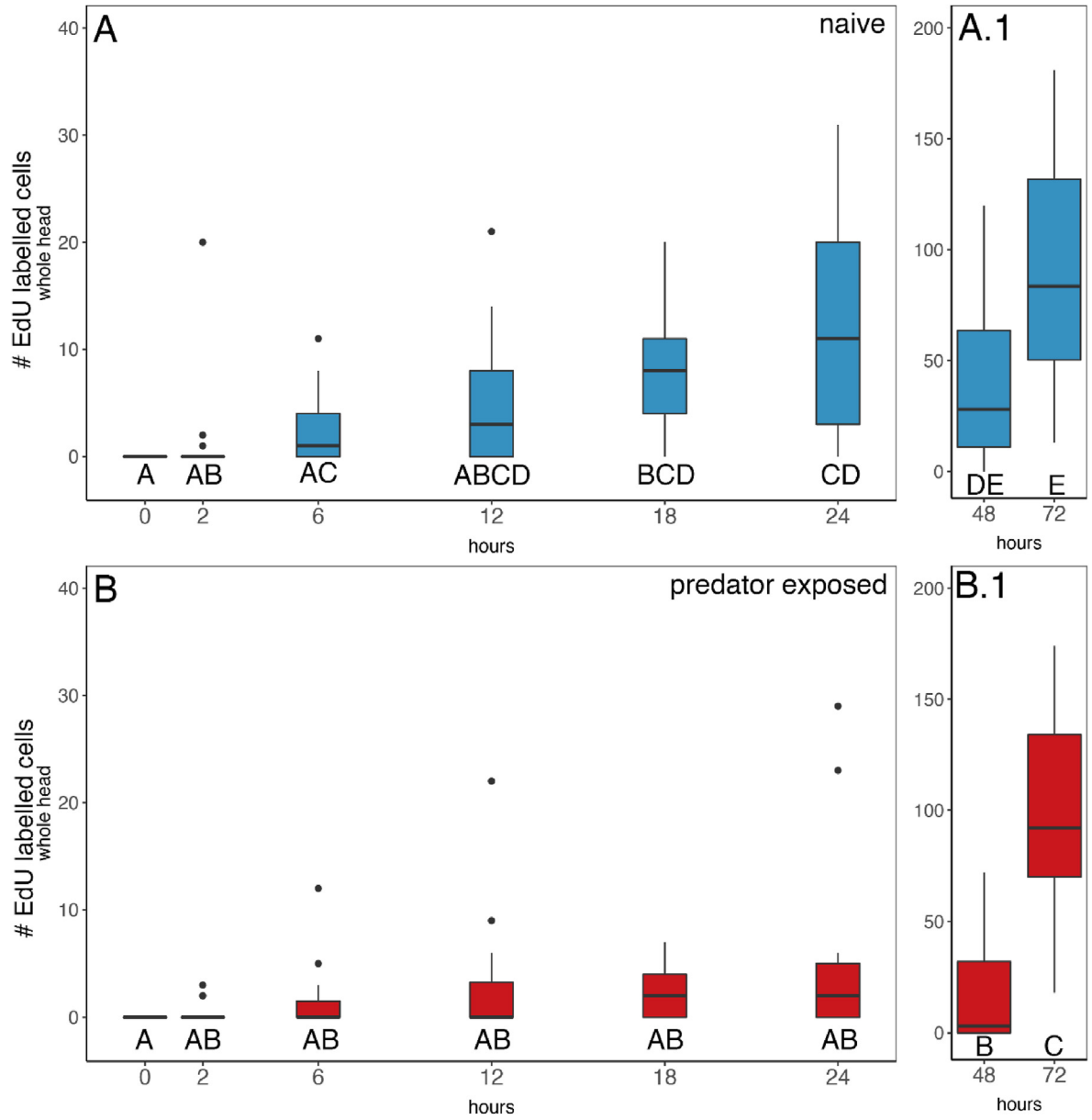

Figure 3. Number of EdU-labeled cells in the whole head tissue of naïve (blue) and predator-exposed (red) *D. longicephala* after 0, 2, 6, 12, 24, 48 and 72 h. A: In naïve *D. longicephala* the number of EdU-labeled cells increases over time. with a significant increase at 18 h and later. A.1: 48 h and 72 h with adjusted scaling. B: In predator-exposed *D. longicephala*, the number of EdU-labeled cells increases over time with a significant increase after 48 h of predator exposure. B.1: 48 h and 72 h with adjusted scaling. Boxplots show median (middle line) and 25th to 75th percentiles (box); whiskers show the highest and lowest values within 1.5× the interquartile range (1.5× below the 25th percentile and 1.5× above the 75th percentile). Dots indicate outliers >1.5× the interquartile range. Significantly different groups are distinguished by different letters.

2.3. EdU incorporation pattern in predator-exposed and naïve D. Longicephala head tissues over time

In naïve *D. longicephala*, the number of EdU-labeled cells in the whole head tissue increased over time, and was significantly higher after 18 h compared with 0 h (Figure 3A, Tables S1, S2).

In predator-exposed *D. longicephala,* the number of EdU-labeled cells remained low in the whole head tissue until 48 h predator exposure. After 72 h predator exposure, the number of EdU-labeled cells in the whole head tissue was significantly higher than that at all previous time points (Figure 3B, Tables S3, S4).

2.4. Comparison of EdU incorporation patterns and cell counts in predator-exposed and naïve D. Longicephala head tissue

The number of EdU-labeled cells in the whole head tissue was significantly smaller in predator-exposed compared to naïve individuals after 18 h, 24 h and 48 h (18 h: $U = 45.5$, $P = 0.004$; 24 h: $U = 116.5$, $P = 0.047$; 48 h: $U = 99$, $P = 0.032$). After 72 h, the number of EdU-labeled cells was similar in both treatments (Figure 4A, $U = 129$, $P = 0.304$, all statistics are listed in Table S5) (Figure 5).

Cell counts in predator-exposed and naïve individuals were not significantly different at 0 h in any region of the head (Table S5). After 2

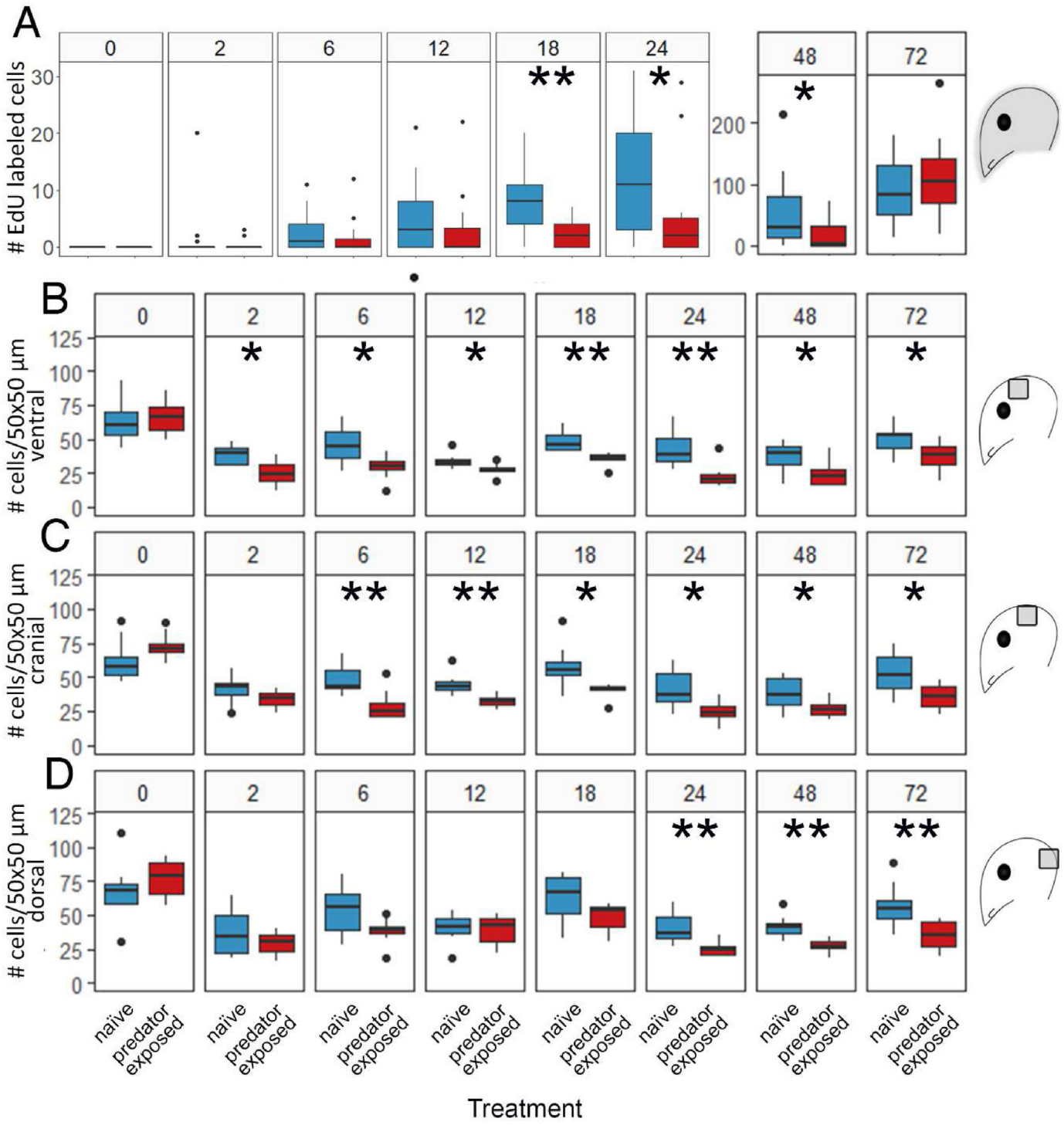

Figure 4. Number of EdU-labeled cells in the whole head tissue and cell counts per 50 × 50 µm of different areas. Naïve *D longicephala* (blue) are compared with kairomone-exposed individuals (red) after 0, 2, 6, 12, 18, 24, 48 and 72 h. A: After 18, 24 and 48 h kairomone exposure, the number of EdU-labeled cells in the whole head tissue was significantly lower compared with the control. 72 h after predator exposure initiation, the number of mitotic cells reaches control levels. B: In the ventral area, we did not find significant differences between treatments after 0 h predator exposure. The cell count is significantly lower after 2 h of kairomone exposure and in all subsequent timepoints compared with the control. C: In the cranial area, the cell count in kairomone-exposed individuals is lower compared with the control after 6 h and at the following timepoints. D: In the dorsal area of the head, cell numbers are significantly lower in kairomone-exposed animals only after 24, 48 and 72 h compared with the control. Boxplots show median (middle line) and 25th to 75th percentiles (box); whiskers show the highest and lowest values within 1.5× the interquartile range (1.5× below the 25th percentile and 1.5× above the 75th percentile). Dots indicate outliers >1.5× the interquartile range. Significant differences are indicated by asterisks (* = $p \leq 0.05$, ** = $p \leq 0.01$, *** = $p \leq 0.001$).

h predator exposure, the number of epidermal cells in the ventral area was significantly lower than in naïve individuals (U = 7.5, $P = 0.012$). In the ventral region, lower cell numbers in predator-exposed individuals persisted throughout all subsequent timepoints (6 h: U = 11, $P = 0.031$; 12 h: U = 9, $P = 0.018$; 18 h: U = 0, $P = 0.001$; 24 h: U = 5, $P = 0.005$; 48 h: U = 13, $P = 0.019$; 72 h: U = 11.5, $P = 0.036$) (Figure 4B, Table S5). In the cranial head region, we detected lower cell numbers in predator-exposed individuals compared to naïve *D. longicephala* from 6 h (6 h: U = 6, $P = 0.007$; 12 h: U = 2.5, $P = 0.002$; 18 h: U = 10, $P = 0.043$; 24 h: U = 9.5, $P = 0.021$; 48 h: U = 16.5, $P = 0.041$; 72 h: U = 11, $P = 0.031$; Figure 4C, Table S5). In the dorsal area of the head, predator-exposed *D. longicephala* showed lower cell numbers compared with naïve individuals after 24 h (Figure 4D, Table S5).

3. Discussion

3.1. Morphological defense expression

Defenses in *D. longicephala* were significantly expressed 48 h after predator exposure and onwards. Before this timepoint defenses in predator-exposed *D. longicephala* were not significantly different to those in the control group, as observed previously (Weiss et al., 2015b). However, tissual defense expression is a consequence of individual cell changes, in which proliferation patterns are regulated upon predator detection. In order to analyze how the cellular responses are transformed into a tissual defense, we investigated cell proliferation patterns in stages prior to and during defense expression.

3.2. Overall EdU incorporation in naïve and predator-exposed D. Longicephala

We found that naïve and predator-exposed *D. longicephala* have distinct patterns of EdU incorporation over 72 h. The constant supply of EdU ensured that newly synthesized DNA was labeled. This meant that the EdU incorporation patterns identified cells that were either in a pre-mitotic (S/G2), mitotic (M) or post-mitotic (G1) phase. Cells that incorporated EdU seem to belong to the class of diploid epidermal cells described by Beaton and Hebert in 1994. In fact, ploidy levels seem to be established by the 1st instar in *Daphnia*, pointing to embryogenesis being the transitional period for the development of endopolyploidy (Neiman et al., 2017). We interpret this to mean that cells that incorporate EdU are very likely to also go through or have gone through mitosis. Of the polyploid cells described by Beaton and Hebert in 1997, which are easily identifiable by their large cytoplasm and extensive nuclei, only one cell of all the stained specimens incorporated EdU. Therefore, we assumed that these bulged cells do not contribute to morphological growth themselves, but potentially only through the agents they release.

In naïve and predator-exposed *D. longicephala,* we detected higher numbers of EdU-labeled cells within the head tissue over time. In naïve *D. longicephala*, these differences became significant at 18 h. Predator-exposed *D. longicephala* showed a remarkably slower cell proliferation rate, and EdU-labeled cells were not significantly increased until 48 h after predator exposure. This is further supported by a direct comparison of EdU-labeled cells between treatments: predator-exposed *D. longicephala* had significantly fewer EdU-labeled cells between 18 h and 48 h compared with naïve animals. Only after 72 h did the cell counts not differ between the two treatments. This indicates that cell cycle progression was delayed and therefore DNA replication and consequent cell division were postponed in the predator-exposed animals until 72 h. This, however, does not directly explain the extensive tissue growth associated with crest expression, which we observed at the 48 h. We therefore hypothesize that cell division was delayed in favor of cell growth, so that the G1 phase in predator-exposed animals may have been prolonged to allow for an extended growth phase of the cells. To analyze cell size, we determined the number of cells identified through nuclear staining in a landmark-specific area. We found fewer cells in predator-exposed *D. longicephala* in all investigated areas. A smaller number of cells within a specific area implies either changes in cell volume or density. As epidermal cells are interconnected by the extracellular matrix (Kruppert et al., 2016; Stevenson, 1985) it is unlikely that the intracellular space increases to reduce cell density. We therefore anticipate that the smaller cell count per selected area over time indicates that the cellular volume (i.e. the proportion between the nucleus and cytoplasm) increases in predator-exposed *D. longicephala*. An initial increase in cellular growth, prolonging the moment of cell division, would not only lead to tissue gain but could also give rise to larger daughter cells after mitosis. Furthermore, crest development could be sped up as the epidermal cells would not go through mitosis, a time-consuming process (Hartwell and Weinert, 1989). Another factor would be uninterrupted cuticle secretion (Minato, 1989). Among *Daphnia* species, *D. longicephala* has been reported to not only express obvious crests but also a structural change in the cuticle, resulting in altered thickness and stiffness (Kruppert et al., 2017; Laforsch et al., 2004; Rabus et al., 2013). In *Chaoborus*-exposed *D. pulex*, Naraki et al. reported the cellular adaptations through which neckteeth are expressed (Naraki et al., 2013). They hypothesized that the epidermal cells in the neck region first divide to form a second layer of cells, where the outer layer excretes the cuticle to build up the neckteeth (Naraki et al., 2013). The cells underneath this cuticle-excreting cell layer then also increase in size, forming the pedestal. Mitotic activity is then also reduced just before the strongest neckteeth expression, suggesting that *D. pulex* postpones mitosis in favor of cell growth and cuticle excretion that build neckteeth. Apparently, the two species use distinct strategies to achieve fast tissue growth to develop crests or pedestals.

To unequivocally show, however, that cells are really dividing and increasing in volume, requires specific antibody staining for validation. For example, EdU is usually combined with an antibody raised against the phosphorylated site of the histone H3 at the serine 10 (H3S10ph). This epitope is only detectable in cells undergoing mitosis (Chen et al., 2018) (or meiosis (Gómez et al., 2016)) and has been used with *Daphnia* cell squashing techniques. To conduct cell size measurements, an antibody that specifically binds to the cells' cytoskeleton like α-tubulin should be used. Unfortunately, such antibody staining in *Daphnia* whole mounts is only possible when removing the impermeable carapace, which was not methodologically possible to combine with the EdU preparations performed here. DNA in the nucleus is replicated during the premitotic S phase (Lemmens and Lindqvist, 2019) so EdU can still be used as an indirect indicator for subsequent mitosis. Therefore, we cautiously interpret the reduced DNA replication rate detected with EdU and reduced cell counts per area as a reduction of mitotic activity combined with an increased cell volume.

3.3. Site-specific proliferation patterns

In general, the site-specific EdU incorporation patterns were similar in each treatment: through visual inspection we detected EdU-labeled cells in the rostrum first and then in the cranial and dorsal directions. The difference between treatments was a delay in this pattern for predator-exposed animals. Therefore, the development of morphological defenses cannot be achieved through altered spatial distribution of cell-division patterns. Such site-specific proliferation patterns have also been reported in *Drosophila* larval growth (Hartenstein and Campos-Ortega, 1985) and other *Daphnia* species (Beaton and Hebert, 1994). Direct comparisons of cell counts in predator-exposed and naïve *D. longicephala* imply that cell volume increase begins in the ventral area within 2 h of predator exposure. At 6 h the cell counts in the cranial region of predator-exposed *D. longicephala* are also significantly different to those in naïve *D. longicephala*. In the dorsal region, significant differences occur after 24 h of predator exposure. This indicates a site-specific and time-dependent proliferation pattern, which could be explained by distinct control pathways, through (i) hormonal control, (ii) controlled

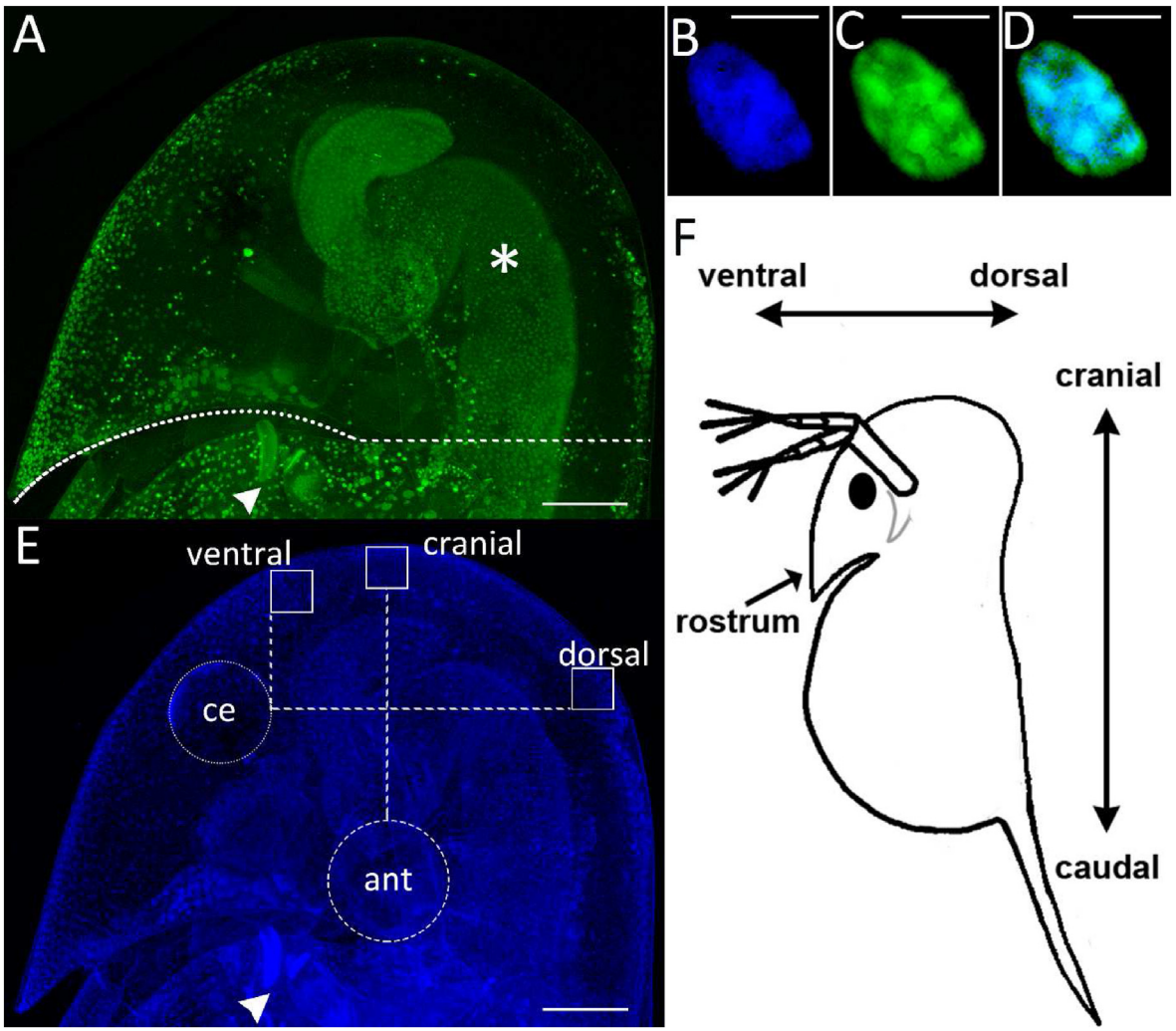

Figure 5. Data acquisition methods. A: Head area in which EdU-labeled cells were counted. Nuclei above the dotted line and labeled with EdU and DAPI were counted, only cells in the intestine (asterisk) were excluded. Arrowhead marks autofluorescence of the *Daphnia* mouthparts. Scale bar, 100 μm. B–D: Nucleus stained with DAPI (B), EdU (C) and an overlay of both (D). Scale bar, 2.5 μm. E: Positions of the three 50 × 50 μm areas used for nuclei counting in the *Daphnia* head. The ventral area was set behind the compound eye (ce), with a vertical line at the posterior eye margin marking the anterior margin of the square. The upper margin of the square was determined by the top of the head. The square in the cranial area was set centrally above the base of the 2nd antenna (ant), with the upper margin being determined by the top of the head. The lower margin of the square in the dorsal area was determined by a horizontal line through the middle of the compound eye. The posterior verge was set at the dorsal margin of the *Daphnia* head. Arrowhead marks autofluorescence of the *Daphnia* mouthparts. Scale bar, 100 μm. F: Orientation in the *Daphnia* body.

release of proliferative agents from certain centers in the vicinity of the morphological defense, or (iii) a combination of both.

Cell proliferation processes are often controlled through hormonal signaling: hormones are released from a specific site and are distributed to the target cells through the hemolymph (Hietakangas and Cohen, 2009; Thompson, 2010). Another explanation for the observed controlled proliferative activity could be the influence of control centers. Beaton and Hebert observed polyploid cells in the vicinity of morphological defenses and proposed that they function as control centers of proliferative activity (Beaton and Hebert, 1997). Later, it was shown that these cells contain the neurohormone dopamine, which in *Daphnia* also increases somatic growth and, in combination with cholinergic agents, even induces morphological defenses (Issa et al., 2020; Weiss et al., 2015a). The proliferating cells in the rostrum that we observed were evenly distributed in the close vicinity of a pair of bulged cells, with a potentially increased ploidy level, which are located near the antennules (Angel, 1967; Weiss et al., 2012b). These seem to control the elongation of the rostrum, which is part of the full defense development. Proliferating cells that were found further in cranial and dorsal direction appeared along the upper margin of the head giving rise to the crest, which is also lined by polyploid cells (Beaton and Hebert, 1997; Weiss et al., 2012b). In the case that these polyploid cells indeed serve as such proliferative centers, the question arises how they are controlled. Until now, no distinct cellular connection to the brain has been found (Weiss, unpublished) to indicate the likelihood of hormonal signaling. It is, therefore, possible that the cell proliferation pattern we observed stems from a combination of hormonal signals together with cell control sites.

Our results indicate that defensive crest expression in *D. longicephala* is based on delayed cell division in favor of increased cellular growth. Cellular adjustments start within the first 2 h of predator exposure and begin in the ventral head region. Subsequently the cranial and dorsal head regions are affected.

4. Materials and methods

4.1. Animal culture

D. longicephala clone LP1 (Lara-Pond, Australia) was cultured in artificial *Daphnia* medium (ADaM (Klüttgen et al., 1994)) in 1 L beakers (Weck®, Germany) containing 20–25 age-synchronized individuals

under constant day:night cycle (16 h:8 h) at 20 ± 1 °C. Animals were fed *ad libitum* with the algae *Acutodesmus obliquus*. The beakers were cleaned every 48 h by removing exuviae and excess algae. Half of the medium was exchanged weekly.

4.2. Kairomone preparation

Notonecta spec., caught in the Botanical Gardens of the Ruhr-University, were kept individually in 1 L beakers filled with pond water and fed daily with 15–20 adult *Daphnia* of different species. Animals were kept under constant day:night cycle (16 h:18 h) in a climatized room at 15 ± 1 °C. Kairomone was prepared 24 h before use: one *Notonecta* was placed into 1 L ADaM and fed every 12 h with 15 adult *D. longicephala*. After 24 h, the *Notonecta* kairomone-enriched ADaM was filtered through a 150 μm mesh. Kairomone-enriched medium was used undiluted in the bioassay.

4.3. Bioassay for cell cycle and nuclei detection

Three-day old *D. longicephala* (3rd juvenile instar) were used in the bioassay. We collected these no more than 12 h after their release from the mother's brood pouch in the 1st juvenile instar from an age-synchronized culture. We chose this instar, because *D. longicephala* is susceptible to *Notonecta* kairomones and significantly expresses defenses within 48 h, i.e. after two moltings in the 5th instar (Weiss et al., 2015b).

For the detection of cell proliferation, we used the reagent Click-iT™ 5-ethynyl-2′-deoxyuridine (EdU) Alexa Fluor™ 488 (ThermoFisher Scientific), which is a non-antibody-based method to detect newly synthesized DNA. This is based on the incorporation of the nucleoside analog EdU, which contains an alkyne in the S-phase of the cell cycle. In a copper-catalyzed reaction, the alkyne reacts with a dye-labeled azide, forming a stable covalent bond. The small size of the azide reagent allows efficient access to the DNA without the need for harsh cell treatment, which enabled us to apply directly to live *Daphnia*. As we continuously applied EdU, this means that it is incorporated in nuclei during the S phase (prior mitosis) of the cell cycle, maintains throughout mitosis (M-phase) and will then also be visible in the daughter cells that subsequently enter G1. The staining pattern observed therefore shows all cells before, during and after mitosis, i.e. all cells that are proliferating. *Daphnia* were placed in 24-well cell culture plates (VWR, Germany). Each well contained one 3rd instar *Daphnia* in 1.5 mL *Notonecta* kairomone or 1.5 mL ADaM as control. EdU was added to a final concentration of 20 μM. *Daphnia* were fed *ad libitum* with *Acutodesmus obliquus* and kept at 20 ± 0.1 °C under constant day:night conditions (16 h:8 h) for 0, 2, 6, 12, 24, 48 or 72 h. To ensure sufficient EdU exposure in treatments that exceeded 12 h exposure length, 500 μL kairomone or ADaM with an EdU concentration of 20 μM was added every 12 h. Animals collected at the respective timepoints, were fixed in 4% formaldehyde (JT Baker, Germany) diluted in phosphate-buffered saline (PBS, 0.1 mol L^{-1}; pH 7.4) for 30 min and dissected as whole mounts by removing one of the 2nd antennae and its base with fine forceps. This left a hole in the carapace that allowed perfusion with the staining reagent for EdU detection. EdU detection was performed according to the manufacturer's protocol. Upon fixation, specimens were washed 3 × 5 min in 3% bovine serum albumin (BSA) diluted in PBS and then incubated in 0.5% Triton®X-100 in PBS for 20 min at room temperature for permeabilization. Next, the permeabilization buffer was removed and *Daphnia* were washed 3 × 5 min in 3% BSA diluted in PBS. Subsequently, the Click-iT® reaction cocktail was added, and specimens were incubated at room temperature under constant shaking and protected from light. Subsequently, specimens were washed 3 × 5 min in 3% BSA diluted in PBS. Specimens were mounted on object slides in VECTASHIELD® Antifade Mounting Medium with DAPI (Vector Laboratories, Burlingame CA) and cover-slipped as described by Weiss et al. (2012).

4.4. Data acquisition

4.4.1. Morphological parameters

First, we analyzed the timepoint of morphological defense expression. Because we know from previous experiments that the animals molt once within ~24 h (Weiss et al., 2015b, Graeve et al., 2021) and crests are significantly expressed after two moltings i.e. ~48 h after predator exposure, we monitored crest development covering three molting cycles i.e. over a time period of 72 h, starting at 24 h after predator exposure and at 48 h after predator exposure.

The fixed animals were photographed to measure the expression of defensive features using the DP74 digital camera mounted on a stereomicroscope (Olympus, SZX16) controlled with the software cell sense (Olympus). We measured crest height as the maximal extension from the upper eye to the most anterior margin of the crest. Crest width was determined as the distance between the dorsal eye margin and the most dorsal extension of the crest, perpendicular to the measurement of the crest height (Weiss et al., 2015b).

4.4.2. EdU incorporation patterns

The number of EdU-incorporating cells was determined in the whole head tissue. We counted EdU labeled nuclei directly under a fluorescence microscope, using 40× magnification (Figure 1A). EdU staining was validated by DAPI colocalization (Figure 1B–D). A minimum of 13 and a maximum of 24 individuals were examined per sampling point and treatment.

4.4.3. Cell density

To investigate the cell density pattern, we determined cell numbers in different head areas, by counting the DAPI-labeled nuclei in squares of 50 × 50 μm. A minimum of 7 and a maximum of 10 individuals were examined per sampling point and treatment.

Specimens were photographed under a fluorescence microscope (Zeiss, Axiophot) (XC10 Olympus + CellSens) with 40× magnification (Plan Apo oil immersion, Olympus) in each area of interest. Afterwards, 50 × 50 μm squares according to the scale of the images were overlayed and nuclei within this square were counted using FIJI (Schindelin et al., 2012). We focused on three areas (ventral, cranial, dorsal; displayed in Figure 1E, F) of the *Daphnia* head to conduct the cell counts. Positions were identified using landmarks, so that the anterior margin of the square in the ventral area was adjusted by superimposing a vertical line at the posterior eye margin. The upper margin of the square was delimited by the top of the head. The square in the cranial area was set above the base of the 2nd antenna, with the upper margin being defined by the top of the head. The lower margin of the square in the dorsal area was defined by a horizontal line through the middle of the compound eye. The posterior verge was set at the dorsal margin of the *Daphnia* head (Figure 1E, F).

4.4.3. Statistics

Morphological data of crest height and crest width followed a normal distribution and we compared the naïve and predator-induced group per point in time (24 h, 48 h and 72 h) using Student's t-test.

We compared the total number of EdU-labeled cells within predator-exposed or naïve *D. longicephala* in the whole head tissue at 0, 2, 6, 12, 24, 48 and 72 h. In addition, we compared the numbers of EdU-labeled cells at each sampling point between the two treatments. Furthermore, we compared cell counts in three different areas in the head of naïve and predator-exposed *D. longicephala* within each sampling point. We tested the count data for a normal distribution using a Shapiro–Wilk test. As data did not follow a normal distribution, the Kruskal–Wallis test and Dunn's multiple comparisons of mean ranks were performed to compare data of all sampling points within naïve or predator-exposed individuals. The Mann–Whitney U test was used to compare naïve and predator-

exposed animals within a single sampling point. All statistical analyses were performed with Statistica 14 (Statsoft Inc.). Diagrams were created with RStudio using the ggplot2 package (R Development Core Team, 2011; Wickham et al., 2016).

Declarations

Author contribution statement

Linda Carolin Weiss: Conceived and designed the experiments; Analyzed and interpreted the data; Wrote the paper.

Annette Graeve: Performed the experiments; Analyzed and interpreted the data; Wrote the paper.

Joshua Huster, Deria Görl and Ioanna Ioannidou: Performed the experiments.

Rocio Gómez: Conceived and designed the experiments; Wrote the paper.

Funding statement

Dr Linda Carolin Weiss was supported by Deutsche Forschungsgemeinschaft [WE6019/2-1].

Data availability statement

Data will be made available on request.

Declaration of interest's statement

The authors declare no conflict of interest.

Additional information

Supplementary content related to this article has been published online at https://doi.org/10.1016/j.heliyon.2022.e10513.

Acknowledgements

We thank Dr. Sebastian Kruppert for statistical and technical advice. Additionally, we acknowledge Elli Buschtöns for maintenance of the animal culture.

References

Angel, M.V., 1967. A histological and experimental approach to neurosecretion in Daphnia magna. In: Neurosecretion.

Baker, G.F., Tortora, G.J., Nostakos, N.P.A., 1976. Principles of anatomy and physiology. Am. J. Nurs.

Barry, Michael J., 2000. Inducible defences in *Daphnia*: responses to two closely related predator species. Oecologia.

Barry, M.J., Bayly, I., 1985. Further studies on predator induction of crests in Australian *Daphnia* and the effects of crests on predation. Mar. Freshw. Res. 36, 519.

Beaton, M.J., Hebert, P.D.N., 1997. The cellular basis of divergent head morphologies in *Daphnia*. Limnol. Oceanogr.

Beaton, M.J., Hebert, P.D.N., 1994. Patterns of DNA synthesis and mitotic activity during the intermoult of *Daphnia*. J. Exp. Zool. 268, 400–409.

Chen, L., Barnett, R.E., Horstmann, M., Bamberger, V., Heberle, L., Krebs, N., Colbourne, J.K., Gómez, R., Weiss, L.C., 2018. Mitotic activity patterns and cytoskeletal changes throughout the progression of diapause developmental program in *Daphnia*. BMC Cell Biol. 19, 30.

Dodson, S.I., Tollrian, R., Lampert, W., 1997. *Daphnia* swimming behavior during vertical migration. J. Plankton Res.

Gómez, R., Van Damme, K., Gosálvez, J., Morán, E.S., Colbourne, J.K., 2016. Male Meiosis in Crustacea: Synapsis, Recombination, Epigenetics and Fertility in *Daphnia magna*. Chromosoma.

Graeve, A., Ioannidou, I., Reinhard, J., Görl, D.M., Faissner, A., Weiss, L., 2021a. Brain volume increase and neuronal plasticity underly predator-induced morphological defense expression in *Daphnia longicephala*. Sci. Rep. 11.

Graeve, A., Janßen, M., Villalba De La Pena, M., Tollrian, R., Weiss, L.C., 2021b. Higher, faster, better: maternal effects shorten time lags and increase morphological defenses in *Daphnia lumholtzi* offspring generations. Front. Ecol. Evol. 9, 324.

Grant, J.W.G., Bayly, I.A.E., 1981. Predator induction of crests in morphs of the *Daphnia carinata* King complex. Limnol. Oceanogr.

Hartenstein, V., Campos-Ortega, J.A., 1985. Fate-mapping in wild-type *Drosophila melanogaster* - I. The spatio-temporal pattern of embryonic cell divisions. Wilhelm Roux's Arch. Dev. Biol.

Hartwell, L.H., Weinert, T.A., 1989. Checkpoints: controls that ensure the order of cell cycle events. Science 80.

Hietakangas, V., Cohen, S.M., 2009. Regulation of tissue growth through nutrient sensing. Annu. Rev. Genet.

Horstmann, M., Topham, A.T., Stamm, P., Kruppert, S., Colbourne, J.K., Tollrian, R., Weiss, L.C., 2018. Scan, extract, wrap, compute—a 3D method to analyse morphological shape differences. PeerJ 1–20.

Issa, S., Gamelon, M., Ciesielski, T.M., Vike-Jonas, K., Asimakopoulos, A.G., Jaspers, V.L.B., Einum, S., 2020. Dopamine mediates life-history responses to food abundance in *Daphnia*. Proc. R. Soc. B Biol. Sci.

Jeschke, J.M., Laforsch, C., Tollrian, R., 2008. Animal prey defenses. In: Encyclopedia of Ecology, Five-Volume Set, p. 189.

Klüttgen, B., Dülmer, U., Engels, M., Ratte, H.T., 1994. ADaM, an artificial freshwater for the culture of zooplankton. Water Res. 28, 743–746.

Krueger, D.A., Dodson, S.I., 1981. Embryological induction and predation ecology in *Daphnia pulex*. Limnol. Oceanogr.

Kruppert, S., Horstmann, M., Weiss, L.C., Schaber, C.F., Gorb, S.N., Tollrian, R., 2016. Push or Pull? The light-weight architecture of the *Daphnia pulex* carapace is adapted to withstand tension, not compression. J. Morphol.

Kruppert, S., Horstmann, M., Weiss, L.C., Witzel, U., Schaber, C.F., Gorb, S.N., Tollrian, R., 2017. Biomechanical properties of predator-induced body armour in the freshwater crustacean *Daphnia*. Sci. Rep. 7.

Laforsch, C., Ngwa, W., Grill, W., Tollrian, R., 2004. An acoustic microscopy technique reveals hidden morphological defenses in *Daphnia*. Proc. Natl. Acad. Sci. U.S.A.

Lemmens, B., Lindqvist, A., 2019. DNA replication and mitotic entry: a brake model for cell cycle progression. J. Cell Biol.

Macháček, J., 1991. Indirect Effect of Planktivorous Fish on the Growth and Reproduction of *Daphnia Galeata*. Hydrobiologia.

Matthews, H.K., Bertoli, C., de Bruin, R.A.M., 2022. Cell cycle control in cancer. Nat. Rev. Mol. Cell Biol. 23, 74–88.

Minato, K., 1989. Cell cycle in the epidermis during larval instars of the Saturniid Moth *Samia cynthia ricini* (Lep.). Zool. Sci. (Tokyo) 6, p35–44.

Miyakawa, H., Imai, M., Sugimoto, N., Ishikawa, Y., Ishikawa, A., Ishigaki, H., Okada, Y., Miyazaki, S., Koshikawa, S., Cornette, R., Miura, T., 2010. Gene up-regulation in response to predator kairomones in the water flea, *Daphnia pulex*. BMC Dev. Biol.

Miyakawa, H., Sato, M., Colbourne, J.K., Iguchi, T., 2015. Ionotropic glutamate receptors mediate inducible defense in the water flea Daphnia pulex. PLoS One 10, 1–12.

Naraki, Y., Hiruta, C., Tochinai, S., 2013. Identification of the precise kairomone-sensitive period and histological characterization of necktooth formation in predator-induced polyphenism in *Daphnia pulex*. Zool. Sci. (Tokyo) 30.

Neiman, M., Beaton, M.J., Hessen, D.O., Jeyasingh, P.D., Weider, L.J., 2017. Endopolyploidy as a potential driver of animal ecology and evolution. Biol. Rev. 92, 234–247.

O'Brien, W.J., Vinyard, G.L., 1978. Polymorphism and predation: the effect of invertebrate predation on the distribution of two varieties of *Daphnia carinata* in South India ponds. Limnol. Oceanogr. 23, 452–460.

Oda, S., Kato, Y., Watanabe, H., Tatarazako, N., Iguchi, T., 2011. Morphological changes in *Daphnia galeata* induced by a crustacean terpenoid hormone and its analog. Environ. Toxicol. Chem.

R Development Core Team, R., 2011. R: A Language and Environment for Statistical Computing. R Foundation for Statistical Computing.

Rabus, M., Söllradl, T., Clausen-Schaumann, H., Laforsch, C., 2013. Uncovering ultrastructural defences in *Daphnia magna* - an interdisciplinary approach to assess the predator-induced fortification of the carapace. PLoS One 8.

Schindelin, J., Arganda-Carreras, I., Frise, E., Kaynig, V., Longair, M., Pietzsch, T., Preibisch, S., Rueden, C., Saalfeld, S., Schmid, B., Tinevez, J.Y., White, D.J., Hartenstein, V., Eliceiri, K., Tomancak, P., Cardona, A., 2012. Fiji: an open-source platform for biological-image analysis. Nat. Methods.

Stevenson, R.J., 1985. Dynamics of the Integument. In: Mantel, L., Bliss, D.E. (Eds.), The Biology of Crustacea. Academic Press, New York.

Stibor, H., Luning, J., 1994. Predator-induced phenotypic variation in the pattern of growth and reproduction in *Daphnia hyalina* (Crustacea: cladocera). Funct. Ecol.

Thompson, B.J., 2010. Developmental control of cell growth and division in *Drosophila*. Curr. Opin. Cell Biol.

Tollrian, R., 1993. Neckteeth formation in *Daphnia pulex* as an example of continuous phenotypic plasticity morphological effects of *Chaoborus* kairomone concentration and their quantification. J. Plankton Res. 15, 1309–1318.

Tollrian, R., 1990. Predator-induced helmet formation in *Daphnia cucullata* (Sars). Arch. Hydrobiol. 119, 191–196.

Tollrian, R., Dodson, S.I., 1999. Inducible Defenses in Cladocera: Constraints, Costs and Multipredator Environments. In: The Ecology and Evolution of Inducible Defenses. Princeton University Press, Princeton, pp. 177–202.

Tollrian, R., Harvell, C.D., 1999. The Ecology and Evolution of Inducible Defenses.

Weiss, L.C., Kruppert, S., Laforsch, C., Tollrian, R., 2012a. *Chaoborus* and *Gasterosteus* anti-predator responses in *Daphnia pulex* are mediated by independent cholinergic and gabaergic neuronal signals. PLoS One 7.

Weiss, L.C., Leese, F., Laforsch, C., Tollrian, R., 2015a. Dopamine is a key regulator in the signalling pathway underlying predatorinduced defences in *Daphnia*. Proc. R. Soc. B Biol. Sci.

Weiss, L.C., Leimann, J., Tollrian, R., 2015b. Predator-induced defences in *Daphnia longicephala*: location of kairomone receptors and timeline of sensitive phases to trait formation. J. Exp. Biol. 218, 2918–2926.

Weiss, L.C., Tollrian, R., 2018. Predator Induced Defenses in Crustacea. In: Welborn, G., Thiel, M. (Eds.), The Natural History of Crustacea: Life Histories, 5. Oxford University Press, pp. 303–321.

Weiss, L.C., Tollrian, R., Herbert, Z., Laforsch, C., 2012b. Morphology of the *Daphnia* nervous system: a comparative study on *Daphnia pulex, Daphnia lumholtzi,* and *Daphnia longicephala*. J. Morphol. 273, 1392–1405.

Wickham, H., Chang, W., Henry, L., Pedersen, T.L., Takahashi, K., Wilke, C., Woo, K., Yutani, H., Dunnington, D., 2016. Springer-Verlag, New York.

Zhang, H., Stallock, J.P., Ng, J.C., Reinhard, C., Neufeld, T.P., 2000. Regulation of cellular growth by the *Drosophila* target of rapamycin dTOR. Genes Dev.